The Lions Gate Bridge – seismic retrofit of north approach viaduct foundations

Li Yan, Ph.D., P.Eng.
Senior Geotechnical Engineer, BC Hydro, Burnaby, BC (formerly with Klohn Crippen Consultants Ltd.).

Alex Sy, Ph.D., P.Eng.
Vice President, Geoenvironment, Klohn Crippen Consultants Ltd., Richmond, BC.

ABSTRACT: The Lions Gate Suspension Bridge in Vancouver, British Columbia, has recently undergone a replacement of the main span deck and seismic retrofit of its north approach. This is believed to be the first design-build seismic retrofit of a major bridge structure in North America. The north approach viaduct is 670 m long and is supported on 24 bents founded on shallow spread footings in gravel deposits. This paper presents the geotechnical aspects of the seismic retrofit design and construction of the north approach viaduct bent foundations. The work consisted of site investigation, liquefaction assessment using the Becker penetration tests, ground deformation analysis, retrofit design and construction. The retrofit consisted of new grade beams to connect individual footings of each bent to minimize differential footing movements, and pile foundation to transfer footing loads below liquefiable soil at bents where large footing movements due to soil liquefaction were predicted. An innovative technique was used to successfully install concrete filled steel pipe piles in coarse sand and gravel deposits to achieve the required pile capacity, with no adverse effect on the existing bent footings.

Introduction

The Lions' Gate Suspension Bridge is one of the landmark structures in Vancouver, British Columbia, and spans the First Narrows of the Burrard Inlet (see location plan in Fig. 1). Connecting Stanley Park in downtown Vancouver to North Vancouver and West Vancouver, the bridge provides a vital transportation link to Vancouver's North Shore communities. After 60 years of service, the bridge underwent a replacement of the main deck with a wider deck structure, and a seismic upgrade of the north approach. The project was awarded to American Bridge/Surespan Joint Venture (ABSJV) in May 1999 under a design-build contract, and Klohn Crippen Consultants Ltd. provided engineering and construction review services to ABSJV for the seismic upgrade of the north approach viaduct. The scope of Klohn Crippen's services for this project included both structural and geotechnical aspects of the seismic upgrade. This paper discusses the geotechnical aspects of the seismic upgrade; the structural aspects were described in Dowdell and Hamersley (2000).

Existing North Viaduct Foundations

The north approach viaduct is a steel structure supported on 24 bents (16 single bents and 4 double or "H" bents), with a cable bent at the south end of the viaduct and an abutment at the north end, as shown on Fig. 2. Each bent is supported by two legs or columns, with each column sitting on a separate footing, except for Bents 3 and 4 that are jointly supported on a massive anchor block. The cable bent foundations were originally spread footings, but were subsequently strengthened in 1978 with piles to arrest differential settlements. The viaduct bent footings are typically 3 m wide by 5 to 6 m long (parallel to bridge centreline), spaced at a centre-to-centre spacing of 11 m, with an embedment of 1.5 m. The footing bearing pressures are as high as 535 kPa for the cable bent, about 355 kPa for Bent 24, and about 250 kPa for the rest of the bents along the viaduct. The existing ground surface slopes gently from north to south towards the Inlet.

Fig. 1 Location Plan

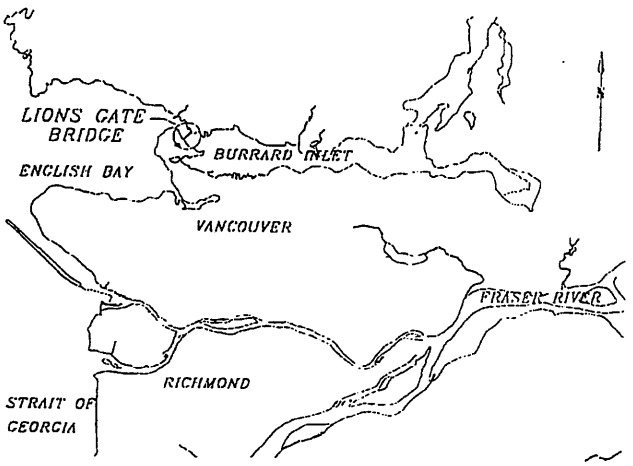

The 15 m high north approach embankment was constructed of gravel fill ranging from sandy soils to boulders of 230 mm size, placed in thin layers and compacted by construction traffic. The finished side slopes of the embankment are 1.5 horizontal to 1 vertical. The north abutment footing of the bridge consists of a base slab 17.4 m by 6.1 m and 0.9 m thick, with an abutment

Fig. 2 Longitudinal View of North Approach Viaduct

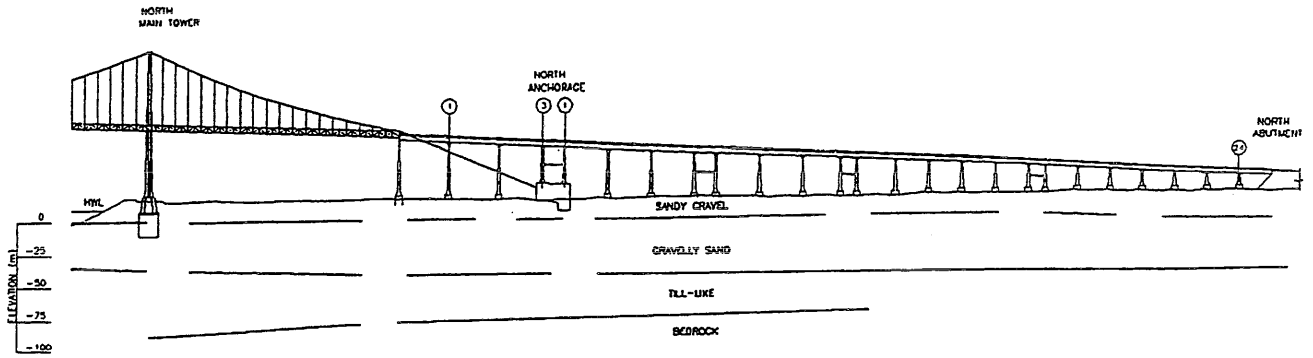

breast wall supporting the northern end of the viaduct deck. The original construction of the Lions Gate Bridge foundations is described in more details in Banks (1942).

Seismic Design Criteria

The design earthquake for this project is a magnitude M7 event with a peak "firm ground" horizontal acceleration of 0.21 g, which corresponds to 1 in 475 year period, or a 10% chance of exceedance in 50 years. Response spectra of the six design earthquake time histories used in the dynamic analyses are shown on Fig. 3. The seismic performance criterion for the north approach viaduct is to ensure that the structure has *limited service* and *repairable damage* after the design earthquake.

Fig. 3 Response Spectra

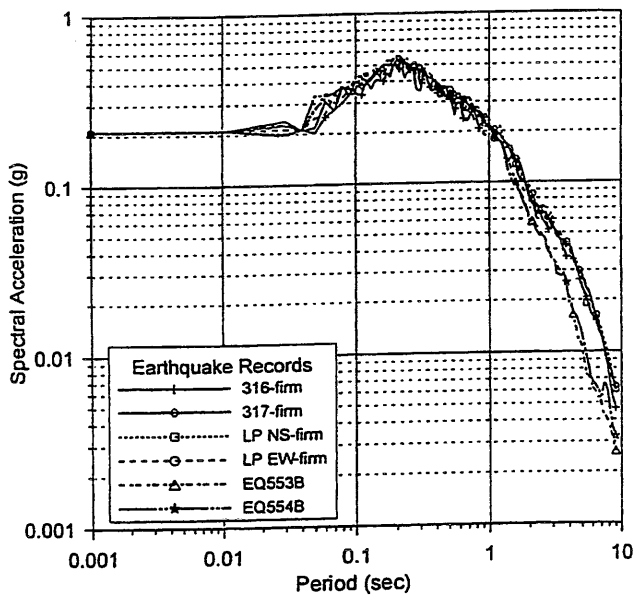

Ground Conditions

Figure 2 shows a simplified soil profile along the north approach viaduct. In general, the north viaduct is underlain by Capilano River deltaic deposits consisting of coarse sands and gravels with some cobbles and boulders to a depth of about 12 to 15 m. The fluvial sand and gravel deposits are generally medium dense, but in some areas, they contain very loose to loose zones. These deposits are underlain by dense sand and silty sand with some gravel to about 55 m depth, which overlie till-like materials comprising very dense sandy silt to very stiff sandy clay with occasional thin layers of gravels and cobbles to about 95 m depth. Underlying the till-like materials is bedrock consisting of mudstone and sandstone. The groundwater levels vary from about 3 to 6 m below grade.

Preliminary liquefaction assessments conducted by the British Columbia Ministry of Transportation and Highways and its consultants had concluded that sporadic soil liquefaction would occur at the north approach viaduct due to the design earthquake, and unacceptable movements could occur at some bent foundations (Naesgaard and Uthayakumar, 1999).

Site Investigation

For the retrofit project, a supplementary site investigation program was conducted by Klohn Crippen in 1999 and consisted of Sonic sampling holes and Becker hammer drill holes. The Sonic drill rig used a top-drive drill head with mechanical vibration and rotation to advance a 108 mm diameter by 3 m long core sampler into the ground for continuous core sampling. During sampling, the Sonic drill hole was cased by a 150 mm diameter steel casing advanced behind the sampler. Water was used as the drilling fluid to advance the casings.

The Becker drill holes, conducted with a model AP 1000 Becker hammer drill rig, consisted of driving a 170 mm outside diameter double-walled casing into the ground, using an ICE 180 double-acting diesel hammer with a rated energy of 11 kJ. The Becker casing was driven both close-ended as a penetration test, and open-ended for sampling, in adjacent test holes. In the Becker penetration test (BPT), blow counts for every 0.3 m of casing penetration were recorded, as well as peak bounce chamber pressure for every hammer blow. In addition, dynamic measurements of the BPT using a Pile Driving Analyzer (PDA) were conducted, and casing friction was also measured with a load cell by pull-up tests at 3 m intervals during each casing add-on (Sy, 1997). For soil sampling, the Becker casing was driven open-ended with compressed air forced down the annulus of the double-walled casing to flush the soil cuttings up the centre of the inner pipe to ground surface, via a cyclone.

The 1999 Sonic and Becker test holes confirmed that the upper sand and gravel deposits (Capilano River sediments) beneath the north viaduct foundations are variable in gradation and density. The deposits are generally medium dense to dense, but contain sporadic zones of very loose to loose sandy and silty materials, with some wood fragments, in the fluvial coarse sand and gravel deposits.

Liquefaction Assessment

Liquefaction resistance of the gravelly soils was estimated from equivalent Standard penetration test (SPT) N_{60} values derived from BPT blow counts. Both the Harder (1988) and Sy (1993) methods of BPT-SPT interpretations were considered. The Harder procedure used peak bounce chamber pressure data with empirical BPT-SPT correlation curve to obtain equivalent SPT N_{60} values from BPT blow counts. In the more fundamental Sy method, the transferred energy data from the PDA and soil friction acting on the casing were used to determine equivalent SPT N_{60} values. The casing friction data were obtained from the casing pull-up tests, and confirmed by CAPWAP analyses of the PDA recorded wave traces (Rausche et al. 1985).

Figure 4 shows measured casing friction data from pull-up tests at twelve BPTs along the north approach viaduct. Although the data points show wide scatter, there is a clear trend of increasing casing friction with depth. In general, the soil friction acting on the 170 mm Becker casing varied from about 50 kN at 3 m depth to about 110 kN at 24 m depth. Also shown on Fig. 4 for comparison is the "average gravel" trend line suggested in Sy (1997).

Fig. 4 BPT Casing Friction Measurements

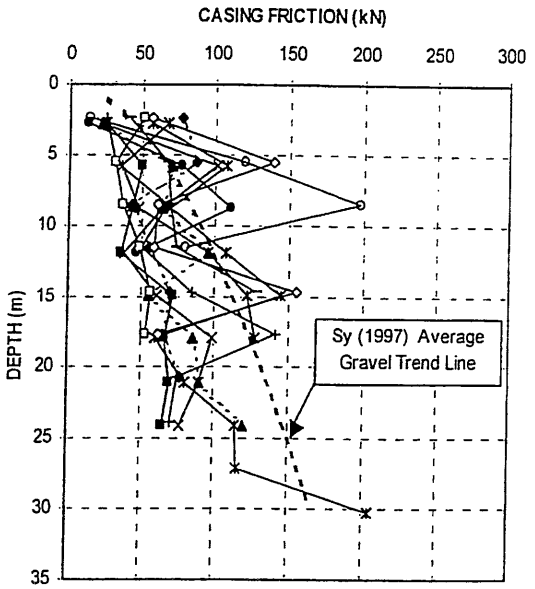

Typical results of equivalent SPT N_{60} values derived from the Harder (1988) and Sy (1993) methods are shown in Fig. 5 for BPT 99-8 conducted near Bent 9. In general, the Sy method gives higher equivalent N_{60} values than the Harder method, except for the loose to very loose zones where similar $(N_1)_{60}$ values were obtained by both methods. The Harder BPT-SPT empirical correlation, based on test data from three sand and silty sand test sites, has embedded casing friction representative of sand and silty sand sites, and therefore can not fundamentally be applied to gravelly soil sites where the casing friction is significantly different (Sy, 1997). The Sy BPT-SPT correlation method explicitly considers site-specific casing friction, and thus is considered to give more representative equivalent SPT N_{60} values of gravelly soils at the north viaduct site.

Induced cyclic shear stresses due to the design earthquake were computed from ground response analyses using the computer program SHAKE91 (Idriss & Sun 1992). Figure 6 shows the peak ground acceleration and effective cyclic shear stress ratio profiles from the SHAKE analyses. The induced cyclic shear stress ratios were then used to compute the SPT N_{60} values required to prevent triggering of liquefaction (i.e. factor of safety against liquefaction = 1.0), using the Seed liquefaction chart (NCEER 1997). The required SPT N_{60} values for the design earthquake are also plotted in Fig. 5 for comparison with the equivalent SPT N_{60} derived from BPT 99-8 at Bent 9. Liquefaction is deemed to occur where the equivalent SPT N_{60} values from the BPTs are lower than the required N_{60} values. It can be seen that the Sy method

Fig. 5 Results of BPT 99-8 at Bent 9

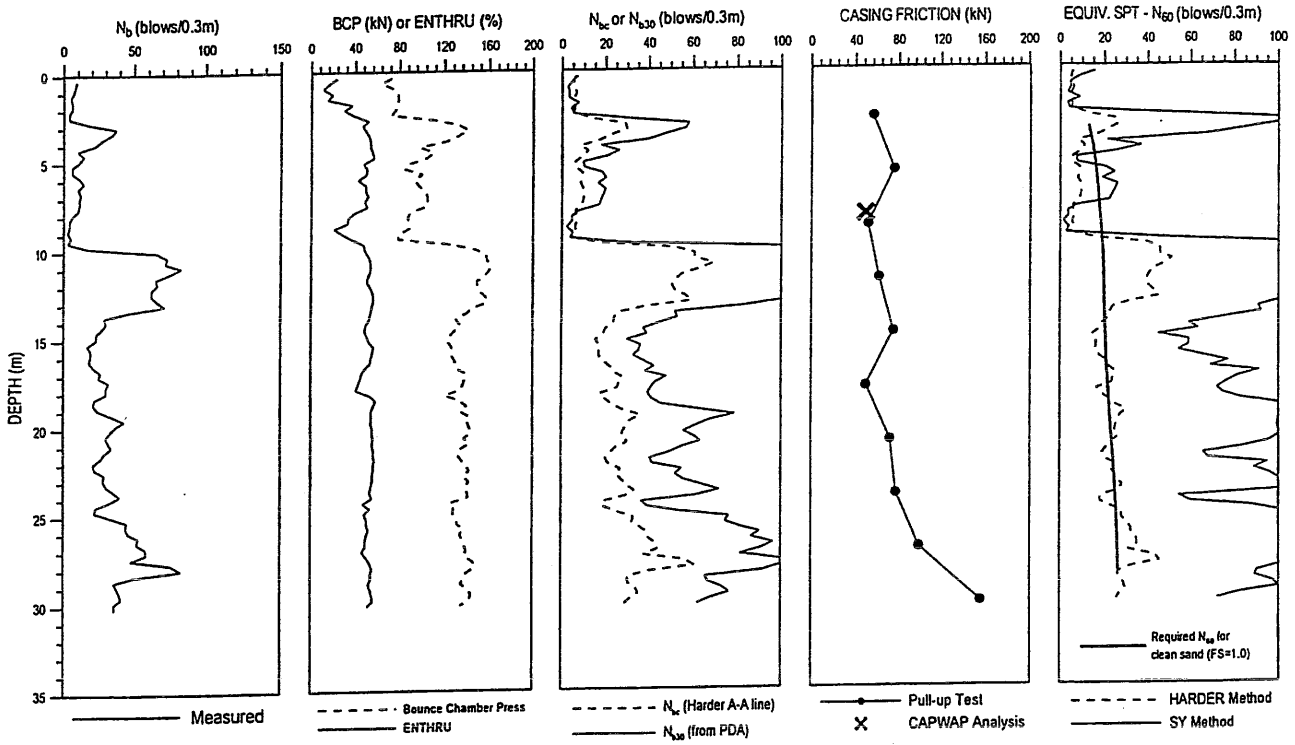

Fig. 6 Results of Ground Response Analyses

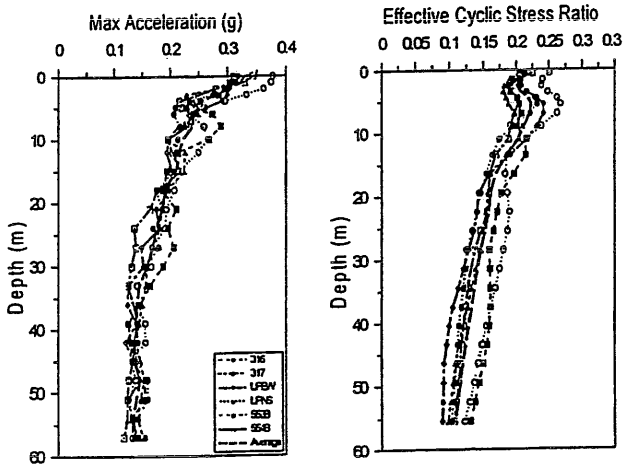

predicts liquefaction in only two localized zones, at 5.2 m and from 7.5 m to 10 m. On the other hand, the Harder method predicts significant liquefaction from 4.5 m to 10 m, and below 14.3 m depth. Similar results were obtained from the other BPTs, with the Harder method indicating significant liquefaction to 30 m depth or more throughout the north approach, and the Sy method indicating localized zones and much smaller extent of liquefaction. It was concluded that without explicitly considering casing friction, the Harder method gave unreasonably low equivalent SPT N_{60} values at this site. Figures 7a and 7b summarize the BPT data and zones of liquefaction predicted by the Sy method along the north viaduct. The drill hole data confirm that the liquefiable zones correspond to the sandy and silty layers which do not extend across the whole site, and suggest that liquefaction will likely be confined to localized loose sandy or silty zones within the fluvial sand and gravel deposits. These loose zones appear to represent low energy environment overbank deposits of the ancient Capilano river channels.

Deformation Analysis

Some of the damaging consequences of soil liquefaction are footing settlements and lateral ground movements. Footing settlements due to foundation soil liquefaction include "undrained settlement" due to soil shear during earthquake shaking and post-earthquake ground settlement due to excess pore pressure dissipation of liquefied soils. The undrained settlement caused by footing shear or bearing capacity failure of the underlying liquefied soil depends not only on the characteristics of the liquefied layers, but also on the footing loads. The drained settlement due to ground re-consolidation depends mainly on the characteristics of the liquefied layers.

Fig. 7a Predicted Zones of Liquefaction (South Half)

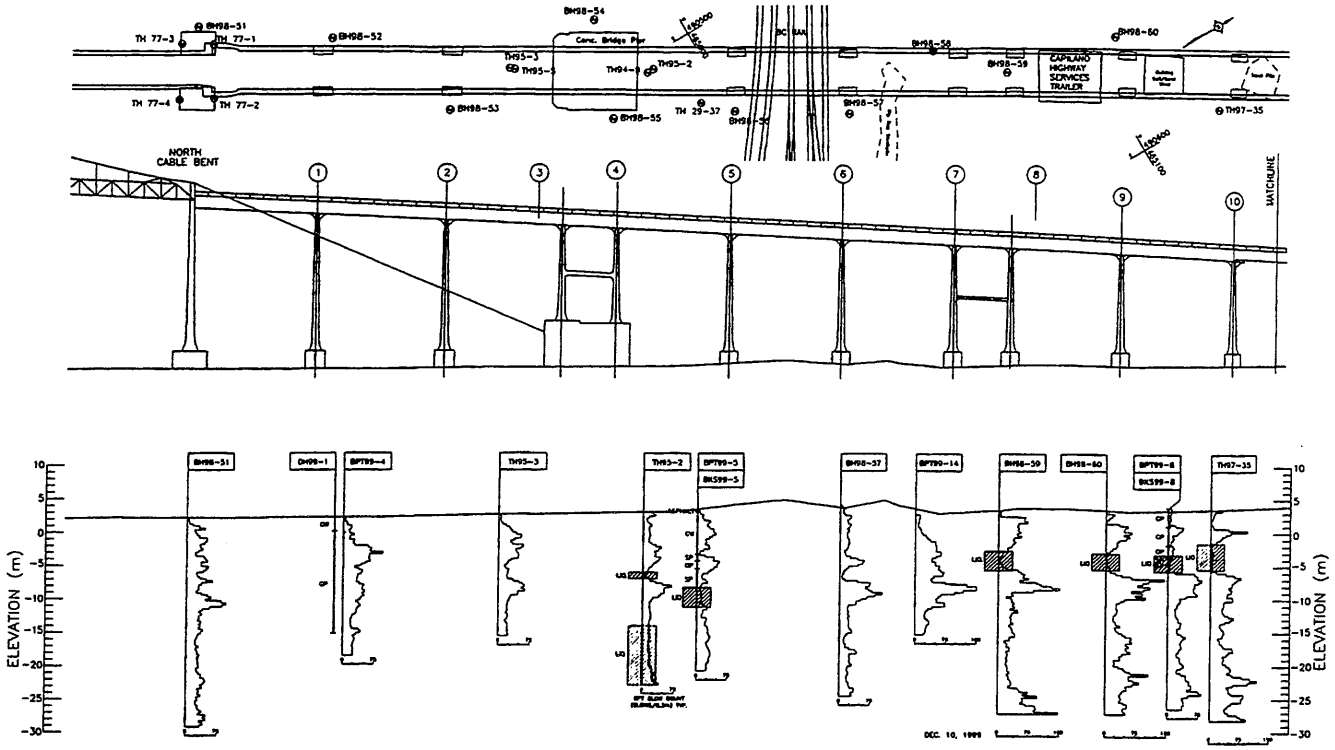

Fig. 7b Predicted Zones of Liquefaction (North Half)

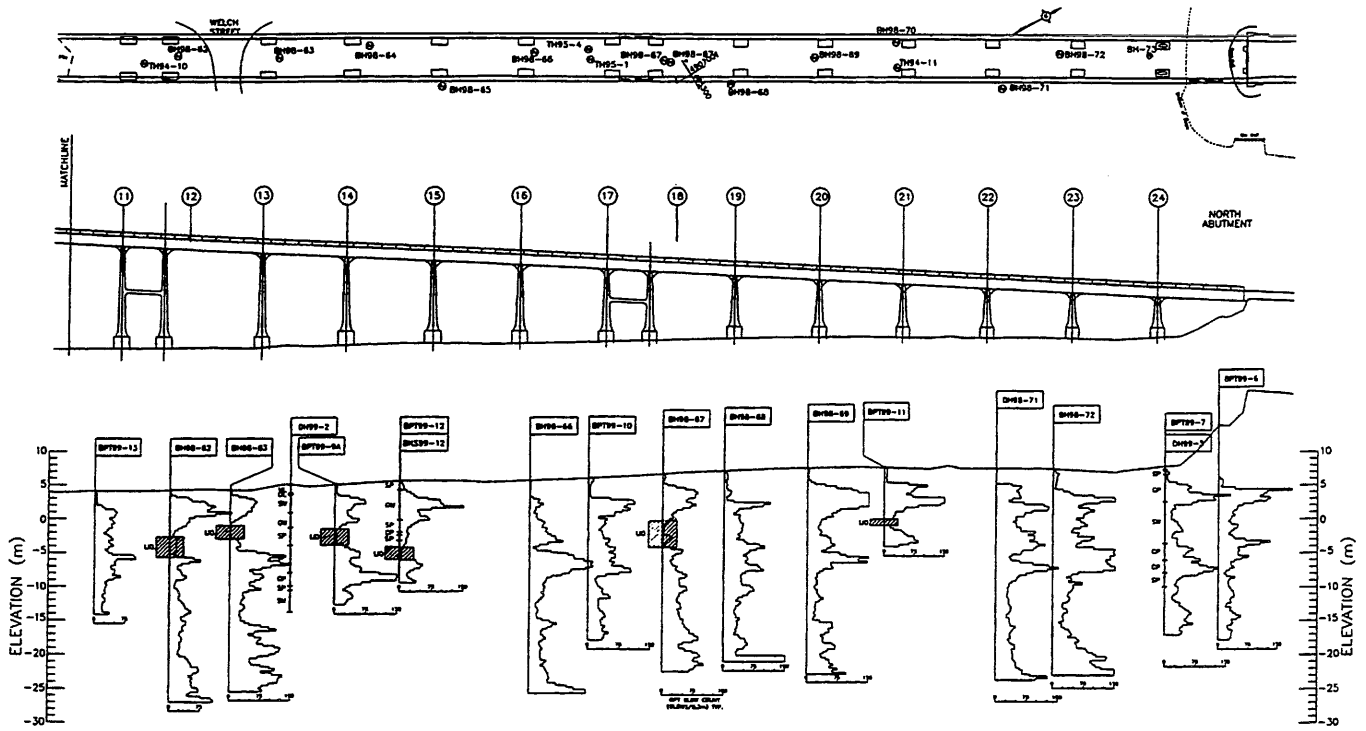

For this project, selected bent foundations were analyzed with the assumed soil parameters shown in Table 1 to assess the magnitude of footing movements due to soil liquefaction at the bent locations, and to confirm the need for foundation remediation.

Table 1 Characteristics of Bents Selected for Deformation Analysis

Bent No.	Depth of Predicted Liquefiable Layer (m)	Design $(N_1)_{60}$ in Liquefied Layer (blows/0.3m)	Design Residual Strength in Liquefied Layer (kPa)
5	11.6 to 14.6	10 – 20	28.8
9	7.5 to 10	5	5
10	5 to 9	5	5
13	6 to 9	5	5
15	9.8 to 11.6	< 5	5
21	7.9 to 8.8	10 – 20	28.8

The undrained footing settlements were analyzed using a 2D plane strain finite difference program FLAC (Itasca 1998) and the drained settlements after earthquake loading were estimated using the procedures proposed by Tokimatsu and Seed (1987), and Ishihara and Yoshimine (1992). In the FLAC analysis, the twin footings of selected bents were modeled, each footing carrying a bearing pressure of 250 kPa, and the soils were simulated using an elastic-plastic Mohr Coulomb stress-strain model. The foundation model consisted of an upper sandy gravel layer to 15 m depth, overlying a gravelly sand stratum to 57 m depth. The predicted liquefied soil layer at the given bent location was included within the sandy gravel layer. The water table was assumed at 3 m below ground surface. The base of the model was taken at the surface of the Pleistocene till deposit at 57 m depth, where the design earthquake ground motion was applied. The footing deformation induced by earthquake shaking was computed with the assumption that soil liquefaction was triggered instantaneously at the time of the peak input motion, and soil strength changed from pre-liquefaction strength to the residual strength of the liquefied soils as shown in Table 1. Typical pattern of footing deformation at the end of earthquake shaking, and the footing settlement time history computed from FLAC analysis of Bent 10 are shown on Figures 8 and 9, respectively.

Fig. 8 Computed Post-Liquefaction Deformation at Bent 10

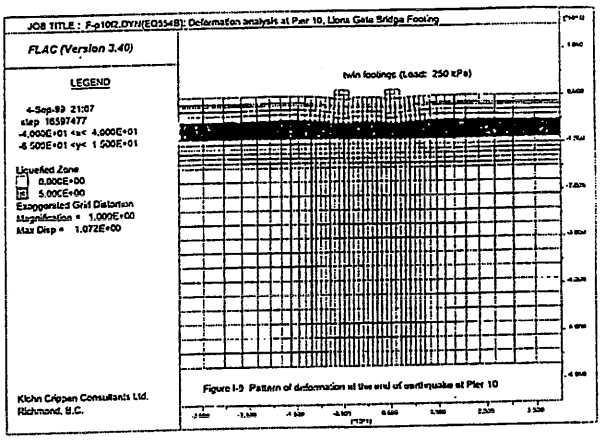

Fig. 9 Computed Settlement Time History of Footing at Bent 10

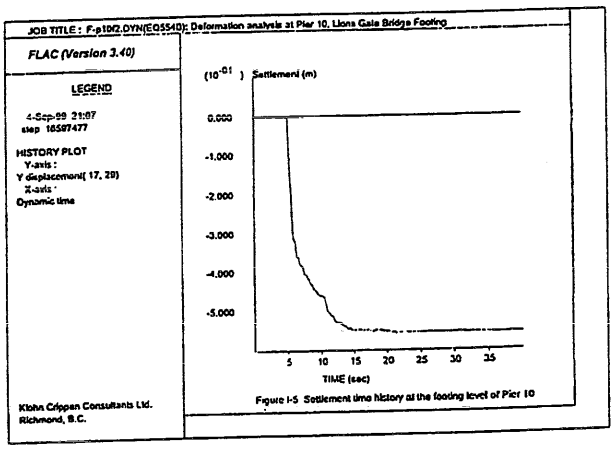

Table 2 summarizes the computed undrained footing settlements from FLAC and post-earthquake consolidation settlements from Tokimatsu and Seed (1987), and Ishihara and Yoshimine (1992) for the selected bents. To check the reliability of the FLAC analysis results, the factors of safety against bearing or punching failure of the footings after soil liquefaction were also calculated using the two-layer formulation proposed by Meyerhof (1974) for a dense sand layer overlying soft clay layer. A friction angle of 35° was assumed for the upper non-liquefied sandy gravel layer, and the undrained residual strengths in Table 1 assigned to the underlying liquefied layer. A footing pressure of 250 kPa was applied in the calculation. As shown in Table 2, the computed factors of safety against footing bearing failure are consistent with the computed undrained settlements from the FLAC model, i.e. low factors of safety for Bents 9, 10 and 13 where large settlements were predicted from shallow liquefied layers, and high factors of safety for Bents 5, 15 and 21 where

small settlements were predicted from deeper, or thinner liquefied layers. Note that for footing design under static loading, a minimum factor of safety of 3.0 is normally used against bearing capacity failure.

Table 2 Summary of Computed Footing Settlements at Selected Bents

Bent No.	Undrained Settlements from FLAC Analyses (mm)	Post-Earthquake Consolidation Settlements (mm)	Factor of Safety against Bearing Failure
5	8 – 28	60	5.2
9	87 – 106	125	2.5
10	345 – 570	200	1.2
13	152 –165	150	1.6
15	33 – 45	90	4.3
21	18 – 22	18	See note [1]

[1] Not determined as liquefiable layer too thin.

The total expected footing settlement due to soil liquefaction under design earthquake loading is the summation of the "undrained settlement" during shaking and "drained settlement" from ground consolidation after earthquake. Based on the results of deformation analyses for the six selected bents, the anticipated total settlements of the other bents were estimated, and the best estimates of total footing settlements for all bents due to the 1 in 475 year design earthquake are shown on Fig. 10. It is seen that the estimated footing settlements are in the range of 180 mm to 605 mm for Bents 8, 9, 10, 12, 13, 14 and 18 that are underlain by relatively thick and shallow liquefied layers. For the other bents where no liquefaction or deeper liquefaction is predicted, the estimated total footing settlements are in the range of 10 to 70 mm, except for Bent 5 and 15, for which the estimated total settlements are 90 mm and 120 mm, respectively.

Because of the generally flat ground surface at the north approach viaduct site, and the sporadic or limited extent of soil liquefaction, earthquake-induced lateral ground movements are expected to be small. The estimated local lateral ground movements range from 0 to 120 mm, based on the empirical data compilation by Bartlett and Youd (1995).

Fig. 10 Estimated Bent Footing Settlements After Design Earthquake

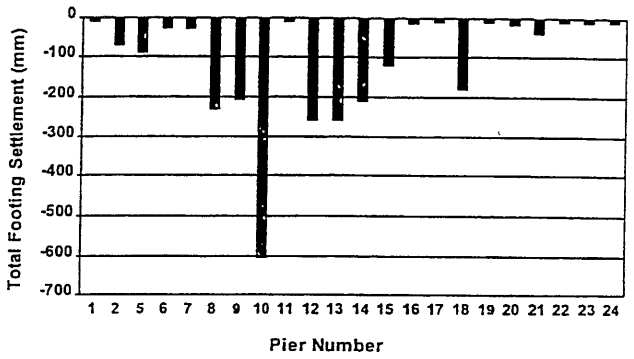

Retrofit Design

The design seismic performance criterion for this project is to ensure that after the 1 in 475 year design earthquake, the north approach viaduct has *limited services*, and *repairable damage*. Therefore, some earthquake induced foundation movements are acceptable provided that the bridge performance criterion is satisfied. The predicted settlements and structural analyses suggest that foundation remediation is required for Bents 8, 9, 10, 12, 13, 14 and 18, where large footing movements are expected due to soil liquefaction between 10 and 15 m depth.

Several foundation remediation options were considered. One of the key criteria was the requirement for the bridge to remain in operation during remediation work, hence the need to ensure that the existing footings were not adversely affected by the work. The remediation option selected was to install low-displacement piles around existing footings to transfer footing axial loads (including negative skin friction from liquefiable soils) to the lower nonliquefied bearing layers, and to resist potential lateral ground movements. The footings at each remediated bent would be enlarged and tied together with horizontal reinforced grade beams to incorporate the remedial piles. For other bents where piles were not required, the existing footings of each bent would also be tied together with horizontal reinforced grade beams to minimize differential footing movements during and after earthquake loading.

The retrofit pile design included consideration of axial pile load capacity, including both footing loads and negative skin friction from the liquefied soil layers, lateral pile response to horizontal ground movements, and pile driveability. For structural analysis of the bridge response to earthquake loading, dynamic stiffness and damping parameters for the bent foundations (both retrofitted and

unretrofitted) were estimated using the computer program DYNA4 (Novak et al. 1993). Figure 11 shows the typical structural bent retrofits, which consist of the addition of diagonal braces in both transverse and longitudinal directions, and the addition of transverse and longitudinal grade beams to tie the footings together (Dowdell and Hamersley, 2000).

Fig. 11 Typical Structural Bent Retrofits

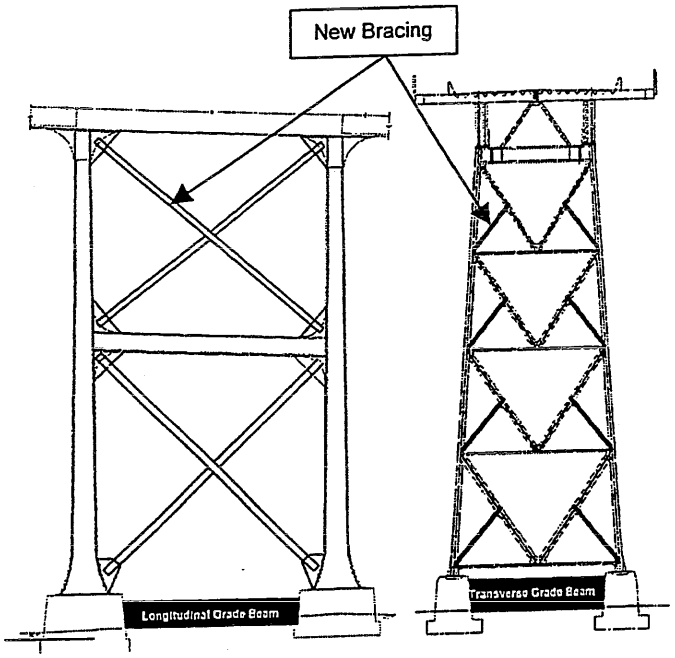

Remedial Pile Construction

Initial H-Pile Test Driving

Low-displacement steel H-piles were initially considered, but there was concern about the ability of the H-piles to penetrate the coarse sand and gravel deposits. A test pile driving program was therefore carried out to evaluate the driveability of steel H-piles at this site. Several HP310x110 test piles, reinforced with cast steel points, were driven, using a 3,400 kg drop hammer. The test piles were terminated at about 3 m depth due to excessive rotation and tilt of pile alignment, and were extracted for inspection. Despite the pile point, all test piles showed evidence of pile toe damage. The observed pile misalignment and pile toe damage were caused by the presence of cobbles and boulders in the granular soils under low confinement at shallow depth, and not by hard driving. It became clear that some form of pre-drilling through the upper coarse materials, combined with much stronger pile toe reinforcement, would be required to successfully install the steel H-piles.

Pipe Pile Installation

After reviewing various pile installation options, concrete-filled steel pipe piles were selected for the foundation remediation. A total of 84 piles were used; 76 piles were 324 mm o.d. by 12.7 mm thick wall steel pipe piles, and the remaining 8 piles were 406 mm o.d. by 12.7 mm thick wall steel pipes. Ultimate axial capacities of 1,110 kN and 1,160 kN were required for the 324 mm o.d. and 406 mm o.d. piles, respectively. A typical pile layout for foundation retrofit is shown on Fig. 12 for Bent 8.

Fig. 12 Remedial Pile Layout

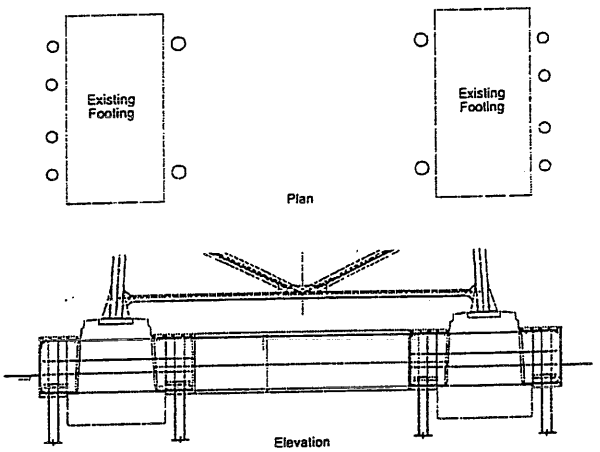

The pipe pile installation procedure was generally as follows:

- Pre-drill to install open-ended steel pipes to 17 m depth to bypass the upper coarse soils and underlying liquefiable layer between 9 m and 15m;
- Remove any soil heave inside the pipes during pre-drilling;
- Tremie concrete to form "plugs" in the pre-drilled pipe sections;
- After concrete is cured, splice piles and drive the piles with an impact hammer to achieve the required design capacity; and
- After pile installation, tremie fill the remaining pipes with concrete.

The pre-drilling was carried out with a Barber drill rig using a 203 mm o.d. downhole hammer and 280 mm o.d. drill bit. A special cutting shoe was welded onto the bottom of the first pipe section. Because the Barber drilling uses compressed air injected at the drill bit to transport soil cuttings to the ground, there was a concern that the drilling process could remove excessive soils from

the ground, especially at depths below groundwater table, causing footing settlements. To minimize soil loss in the ground, the downhole hammer bit was maintained about 150 mm behind the pipe shoe. Soil cuttings during drilling were monitored for volume, and the soil heave inside the pipe at the end of drilling was measured. It was found that the volume of soil cuttings was generally less than the theoretical pipe volume for the first 5 m depth, increasing to about 50% more than the theoretical value below 11m depth. Measured soil heave inside the pipe varied from 0.5 m to 5 m. Despite the ground loss and soil heave inside the pipes, there was no measurable settlement of the bridge bent footings.

Soil heave inside the drilled-in pipes was removed with a bailer using a cable-tool drill rig. During bailing, the pipes were filled with water to minimize further soil heave. After removal of the soil heave, the pre-drilled pipes were filled with 40 MPa tremie concrete. Concrete cylinder samples tested at 7 days confirmed concrete compressive strengths in excess of 40 MPa.

After the concrete had cured and gained sufficient strength, the concrete-filled steel pipe piles were spliced with additional pipe sections and driven with a drop hammer. Pile driving criteria were established using a Pile Driving Analyzer and CAPWAP analyses of the wave traces during impact hammer driving. The CAPWAP results indicated very low soil resistance in the upper 17 m pre-drilled section, and that most of the pile capacity was derived from shaft resistance below about 24 m depth, with little toe resistance. The total static pile capacities estimated from the CAPWAP analyses for the 324 mm diameter piles are plotted against pile embedment as shown on Fig. 13. Based on the CAPWAP results, all piles were driven to either a minimum embedment of 40 m, or to a final set. During impact driving, it was found that the 17 m long concrete plugs formed within the pre-drilled sections of the piles moved up as much as 1.5 to 1.8 m.

Effects on Existing Foundations

Settlement monitoring of existing bent footings was carried out during every phase of pile installation, including pre-drilling, soil heave removal inside steel pipes, and impact driving of the piles. A hydraulic jacking system was also installed on the footings, to be used to jack up the bent columns in the event that excessive footing settlements were to occur during pile installation. No significant settlements of the existing bent footings occurred at the remediated bents due to pile installation.

Fig. 13 Axial Pile Capacities Estimated from CAPWAP Analyses

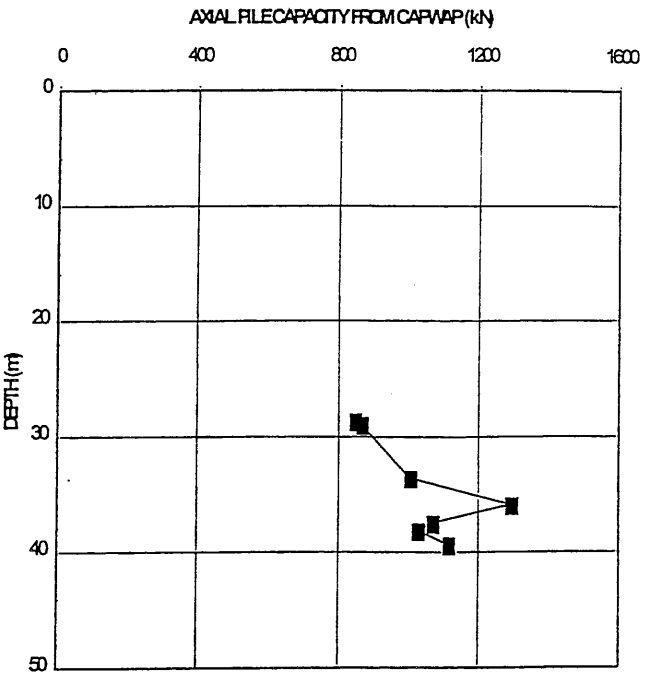

Summary and Conclusions

The north viaduct bent foundations of the Lions Gate Suspension Bridge have been successfully retrofitted for the 1 in 475 year design earthquake. The geotechnical challenges for the seismic retrofit included liquefaction and deformation assessments of bent footings in coarse sand and gravel soils, and implementation of a cost-effective remedial scheme that had minimal impact on the existing pier footings to allow bridge operation during all phases of the foundation retrofit.

Becker hammer drill and Sonic drill holes were used to characterize the subsoil and groundwater conditions, and to delineate discontinuous loose to very loose sandy and silty layers within the fluvial coarse sand and gravel deposits underlying the site. The Seed SPT-based liquefaction method was used in the liquefaction analysis. The liquefaction resistance of the gravelly soils was determined from Becker penetration tests (BPT). BPT-SPT interpretation using the Sy method, which explicitly considers transferred energy and casing friction, provided reasonable estimates of equivalent SPT N_{60} values. Sporadic zones of liquefaction were predicted, associated with localized loose sandy zones in the otherwise medium dense to dense Capilano river sediments.

Footing movements due to soil liquefaction and ground re-consolidation after earthquake shaking were evaluated for all bents. Large settlements were predicted for bent footings underlain by relatively thick and shallow liquefiable layers, and small settlements predicted for bents underlain by deeper or no liquefiable soils. To meet the bridge seismic performance design criteria of limited service and repairable damage, it was decided to upgrade Bents 8, 9, 10, 12, 13, 14 and 18, due to the large predicted movements. In addition, heavily reinforced horizontal grade beams were used to tie together the twin footings of each bent to minimize potential differential movements between footings. Because of the presence of cobbles and boulders in the sand and gravel deposits, an innovative pile installation procedure was used, which combined pre-drilling and impact driving, to install concrete-filled steel pipe piles to provide the required capacity with no measurable adverse effects on the existing footings. The seismic retrofit of the north approach viaduct was performed with bridge in constant operation.

Acknowledgements

The authors wish to acknowledge the contribution of other Klohn Crippen engineers, including Bruce Hamersley, Dave Dowdell, Derrick Kelly, and Dennis Teo, without whose contribution and dedication the project could not have been successfully completed. The authors also thank American Bridge for their great work in completing this challenging design-build seismic retrofit project. Professor Peter M. Byrne of the University of British Columbia provided technical review for this project.

References

Banks, S.R. 1942. The Lions' Gate Bridge parts I, II, III and IV, The Journal of the Engineering Institute of Canada, April, May, June and July.

Bartlett, S.F. and Youd, T.L. 1995. Empirical prediction of liquefaction-induced lateral spread. Journal of Geotechnical Engineering, ASCE, Vol. 121, No. 4, pp.316-329.

Dowdell, D.J. and Hamersley, B.A. 2000. Lions Gate Bridge North Approach – Seismic Retrofit. Proceedings, STESSA 2000, August 21-24, Montreal, Quebec, Canada

Harder, L.F. Jr. 1988. Use of penetration tests to determine the liquefaction potential of soils during earthquake shaking. Ph.D. dissertation, University of California, Berkeley.

Idriss, I.M and Sun, J.I. 1992. User's Manual for SHAKE91, program modified based on the original SHAKE program titled "A computer program for conducting equivalent linear seismic response analyses of horizontally layered soil deposits", University of California, Davis, California.

Ishihara K. and Yoshimine M. 1992. Evaluation of settlements in sand deposits following liquefaction during earthquakes. Soils and Foundations, Vol. 32, No. 1, pp. 173 – 188.

Itasca Consulting Group, Inc. (1998). FLAC – Fast Lagrangian Analysis of Continua Version 3.40. Minnesota, US.

Meyerhof, G.G. 1974. Ultimate Bearing Capacity of Footings on Sand Layer Overlying Clay. Canadian Geotechnical Journal, Vol. 11, No.2, pp.224-229.

Naesgaard, E. and Uthayakumar, M. 1999. Numerical analyses for seismic retrofit design Lions Gate Bridge, Vancouver, British Columbia. FLAC and Numerical Modelling in Geomechanics, Editors: Detournay & Hart.

NCEER 1997. Proceedings of the NCEER workshop on evaluation of liquefaction resistance of soils. Technical Report NCEER-97-0022, December, edited by Youd, TL and Idriss, IM.

Novak et al. 1993. DYNA4 – A computer program for foundation response to dynamic loads. Geotechnical Research Centre, University of Western Ontario.

Rausche, F., Goble, G.G and Likins, G.E. 1985. Dynamic determination of pile capacity. ASCE Journal of Geotechnical Engineering, 111(3):367-383.

Sy, A. 1993. Energy measurements and correlations of the Standard penetration tests (SPT) and the Becker penetration tests (BPT). Ph.D. thesis, Department of Civil Engineering, University of British Columbia, Vancouver, B.C.

Sy, A. 1997. Twentieth Canadian Geotechnical Colloquium: Recent developments in Becker penetration test: 1986 to 1996. Canadian Geotechnical Journal, 34(6):952-973.

Tokimatsu, K. and Seed, H. B. 1987. Evaluation of settlements in sands due to earthquake shaking. Journal of Geotechnical Engineering, ASCE Vol. 113, No. 8, pp. 861-878.